Applied Clay Science 53 (2011) 8–14

Contents lists available at ScienceDirect

Applied Clay Science

journal homepage: www.elsevier.com/locate/clay

Research paper

Improvement of the mechanical strength of alumina preforms by coating with montmorillonite/LDH gels

Mridusmita Mishra, Jayanta Jyoti Bora, Rajib Lochan Goswamee *

Materials Science Division, North-East Institute of Science & Technology (NEIST), (formerly RRL) CSIR, Jorhat, Assam, 785 006, India

ARTICLE INFO

Article history:
Received 25 May 2010
Received in revised form 31 March 2011
Accepted 8 April 2011
Available online 11 May 2011

Keywords:
Layered double hydroxide
Spinel
Dip coating
Ceramic matrix
Alumina tubes
Montmorillonite
Gel

ABSTRACT

A composite material was prepared from montmorillonite and Mg–Al LDH. These oppositely charged particles form thixotropic gels with distinct flow and micro-structural properties. The stability of the gel was dependent on the montmorillonite/LDH ratio. Novel advanced ceramic materials were designed by coating ceramic preforms with these gels. During calcination these gels decompose to metal oxides, aluminosilicates and spinel. On calcination at 1400 °C, MgO formed from the LDH of the gel reacted with the aluminosilicate formed by the decomposition of the montmorillonite. A non-porous dense matrix was formed with well grown crystals of $MgAl_2O_4$ spinel embedded in the aluminosilicate matrix. When the ceramic preforms like porous alumina tube were dip coated with the gel and fired at 1400 °C, the molten aluminosilicate infiltrated into the pores of the aluminum oxide carrying spinel crystals. These spinel crystals settled in the pores and increased the mechanical strength of the alumina tubes. The compressive strength was increased by around 94% and the mechanical extension in the z-direction in the coated body by 4% compared to the uncoated counterpart.

1. Introduction

The thixotropy is a phenomenon, where the viscosity decreases under stress, followed by gradual recovery when the stress is removed (van Olphen, 1977). The viscosity rise is due to gel formation by continuous particle–particle networks as a consequence of weak attractive forces between the particles (Lagaly, 2006). By adding different chemical agents, gelation can be modified to increase or decrease the viscosity. LDH can also work as an inorganic viscosifier for aqueous dispersions of montmorillonite (Abend et al., 1998; Abend and Lagaly, 2000; Lagaly et al., 2001a, 2001b).

The LDH particles have about 150 Å size (Miyata, 1975), possess very high positive charge densities ≈0.04 charges/Å^2, anion exchange capacities (AEC) of ≈2.4 to 4.1 meq/g (Jones and Chibwe, 1989) and a thickness of 0.8 nm (Li et al., 2005). The AEC of LDH is almost three/four times larger than the cation exchange capacity (CEC) of montmorillonite (≈0.7 to 1.0 meq/g). The positively charged LDH particles can strongly interact with the negatively charged montmorillonite particles. Due to this electrostatic interaction between the particles, highly thixotropic dispersions can be formed (Li et al., 2003) which is important in formulating fluids with specific industrial uses (Abend et al., 1998; Burba et al., 1987; Sparling and Williamson, 1991). The montmorillonite–LDH interaction was also the basis to develop novel ceramic devices for environmental applications (Goswamee et al., 2009).

Apart from this, the compositional differences of various LDHs give rise to interesting variations of their thermal behavior by forming a number of oxidic phases like non-stoichiometric oxides (NSO), spinels, and nanometer sized oxide particles (Kovanda et al., 2003). The temperature at which the different oxides form, depends on the composition of the LDH. During calcination, Mg–Al LDH undergoes conversion into a rock-salt type non-stoichiometric mixed metal oxide at around 300 °C. Above 900 °C it begins to form MgO and $MgAl_2O_4$ (Forano et al., 2006 Miyata, 1975;). Such composites when dip-coated on ceramic preforms show interesting properties of the coats at different temperatures.

Dip coating is used to form thin films by using the layer by layer (LBL) deposition on solid substrates. Initially a well defined charged precursor film with a thickness of around 10 nm has to be formed using organic or inorganic polymers like poly(ethylene-di-amine), poly(styrene-sulphonate), aluminum or zirconium (hydr)oxy species etc. upon which the ionic inorganic materials like polyoxometallates (POM), SiO_2 particles, montmorillonite particles or zirconium phosphate exfoliated by tetra-n-butyl ammonium ions are adsorbed (Ariga et al., 1999; Decher et al., 1994; Lagaly, 1999; Li et al., 2005). The films of the layered materials with high lateral bond strength and high aspect ratio function as an ideal planar material for such self assembled film growth through the LBL process.

After coating solid surfaces by montmorillonite/LDH composites, a nano-scale periodicity can be expected in the LBL films as a consequence of strong particle–particle interaction. In this study, the influence of different oxidic phases formed by the thermal decomposition of the coated montmorillonite/LDH gels on the

* Corresponding author. Tel.: +91 376 2370081; fax: +91 376 2370011.
E-mail address: goswamirl@rrljorhat.res.in (R.L. Goswamee).

0169-1317/$ – see front matter © 2011 Elsevier B.V. All rights reserved.
doi:10.1016/j.clay.2011.04.004

mechanical properties of ceramic preforms was studied. The essential steps of coating ceramic preforms with the gels are explained in Fig. 1. These include the steps: preparation of the aqueous gel having a stable flow behavior at proper compositional ratios of the components, coating the preforms with the gel at an optimized dipping and withdrawal sequence, controlled drying of the coated body, and finally calcination.

2. Experimental section

2.1. Materials and methods

2.1.1. Purification and analysis of the bentonite

Commercial grade bentonite was obtained from M/S Loba Chemie India. The <2 μm fraction of the bentonite was obtained by sedimentation (Lagaly, 2006; Lee et al., 2007; Patel et al., 2007). The organic matter was destroyed by boiling in H_2O_2 over a hot water bath. The purified bentonite showed − 11.7% (m/m) loss on ignition at 950 °C and contained 47.5% (m/m) SiO_2, 34.8% (m/m) Al_2O_3, 1.3% (m/m) Fe_2O_3, 2.3% (m/m) CaO, 1.1% (m/m) MgO, 0.4% (m/m) Na_2O, 0.2% (m/m) K_2O and 0.7% (m/m) unidentified materials. The XRD pattern of the oriented purified bentonite, after drying at around 85% relative humidity at 25 °C, showed reflections with d-values of around 15 Å, 4.4 Å and 3.1 Å (Fig. 2A), which resembled closely to JCPDS PDF pattern no. 13–135 for montmorillonite A.

Further purification of the bentonite was carried out by dispersing 14 g of the bentonite fraction (after the decomposition of the organic material) in 200 ml aqueous 1 M NaCl at room temperature under repeated periods of 10 min sonication. The total period of sonication was 100 min during one week. Sonication was carried out at an amplitude of 33% with a 25 mm Titanium horn in a high intensity ultrasonic processor (model VCX 500 from M/S Sonics and Materials Inc., USA). The bentonite dispersion was dialyzed in a dialysis bag (from M/S Sigma Chemicals Co. USA) in distilled water for several weeks. During dialysis the water was constantly changed after each night so that the Na^+ content in the dialyzed water was below 5 ppm. The powder XRD pattern of the air dried Na-montmorillonite showed an intense *(001)* reflection at d = 12.8 Å (Brindley and Brown, 1980). The cation exchange capacity (CEC) of this Na-montmorillonite as determined by ammonium saturation was 0.97 meq/g (Bain and Smith, 1994; Searle and Grimshaw, 1960).

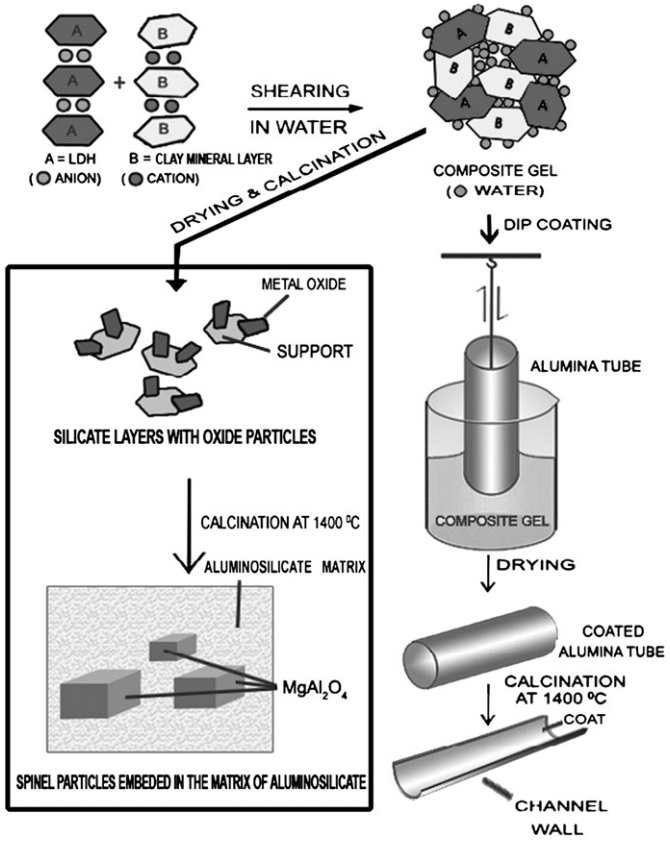

Fig. 1. Coating of alumina supports by composite gels of Mg–Al LDH and Na-montmorillonite.

2.1.2. Preparation and characterization of Mg–Al LDH

Preparation of the Mg–Al LDH was carried out by dissolving 0.75 M $MgCl_2.6H_20$ and 0.225 M $AlCl_3.6H_2O$ in 300 ml water. The solution was added in small droplets to 200 ml solution of NaOH (0.5 M) and Na_2CO_3 (0.02 M) at pH 10 under stirring during 6 h. The dispersion was then agitated in a closed vessel at 65 °C for 24 h, filtered, washed and dried. Chemical analysis indicated a Mg:Al ratio of 3.3.

The CO_3^{2-}content (2.27 meq/g Mg–Al LDH) in the LDH was calculated from the amount of C determined by elemental analysis in a CHN analyser (model M/S Perkin Elmer 2400) at a combustion temperature of 950 °C. To estimate the amounts of Cl^-ions in the interlayer space of Mg-Al LDH, the interlayer Cl^-were initially exchanged with carbonate ions (Goswamee et al., 1998) by reacting 500 mg of the 80 °C air dried Mg-Al LDH with 50 ml 0.06 M Na_2CO_3 solution. The mixture was shaken at room temperature in a rotary shaker for 24 h at 130 RPM. The sediment was filtered through Whatman 41 filter paper and washed several times with diluted Na_2CO_3 solution. The filtrate was evaporated to reduce the volume to 50 ml. The chloride content in the solution was estimated by ion-chromatography (model Metrohm 881 IC Compact Pro1) using the Metrosep A Supp5 anion separation column with a Na_2CO_3 and $NaHCO_3$ mixture as the mobile phase. The Cl^-content was 0.007 meq/g.

The very small amount of exchangeable Cl^-ions in comparison to the large amount of CO_3^{2-}ions in the interlayer is a consequence of the fixing of the CO_3^{2-}ions in the interlayer space of LDHs (Taylor, 1973; von Allman, 1970).The CO_3^{2-}ions were formed from atmospheric CO_2 during the synthesis at alkaline pH. Because of high CO_3^{2-}/Cl^-ratio, the synthesized sample was assigned as Mg–Al–CO_3^{2-}. The empirical formulae of LDH, considering the CO_3^{2-}as the dominant interlayer anions was $[Mg_{3.3}Al\,(OH)_{8.6}](CO_3)_{0.5}xH_2O$ with an AEC of 2.27 meq/g.

The powder XRD of the uncalcined Mg–Al LDH sample gave a pattern with high intensity integral *(001)* reflections along with the *(hkl)* reflections (Fig. 2B). The specific BET surface area of prepared LDH particles as measured by nitrogen adsorption (Quantachrome USA, model Autosorb 1) was 51 m^2/g.

2.1.3. Gel preparation and flow behavior

Aqueous dispersions of 0.5% (m/v) purified Na-bentonite were prepared in a high intensity ultrasonic processor (model VCX 500, from M/S Sonics and Materials Inc., USA) with a one inch solid titanium horn (20 kHz, 33% amplitude, 10 min with 3.5 s pulse on and 1.5 s pulse off mode). Over one week the total time of sonication was 1.5 h. During the one week there was an approximate 18 h gap between each exposure to sonication. To this dispersion, various amounts of finely ground Mg–Al LDH ranging from 0.025% (m/v) to 0.35% (m/v) were added. The dispersions were also sonicated for the 10 min periods exposure steps using the sonicator operating parameters as before. The rheological parameters were measured with the Brookfield LVT–DVII rate controlled viscometer having an UL adapter and co-axial cylindrical geometry as well as with a controlled stress rheometer (Rheolab QC from M/S Anton Paar Ltd) using a spindle and cup combination (model CC27-CC10). The calibration liquid was DKD-k-06901 from M/S Anton Paar Ltd.

2.1.4. Electrokinetic behavior of the gel

The electrokinetic mobility of the Na-montmorillonite and Mg–Al LDH composites at different pH were measured after sonication of the dispersions. An amount of 30 mg gel was dispersed in 50 ml water at varied Mg–Al LDH to montmorillonite ratios. The pH of the dispersions was adjusted by addition of 0.01 M NaOH or 0.01 M HCl. The electrokinetic mobility was measured with the Laser Doppler Velocimetry technique at 25 °C under a 10 mW He–Ne laser (Malvern Instruments Zetasizer 3000-HS).

2.1.5. Thermal behavior

The samples were heated in air at 800, 1000, 1200, 1400 °C for 30 min and cooled to room temperature under normal atmosphere. The phases formed were identified by powder XRD.

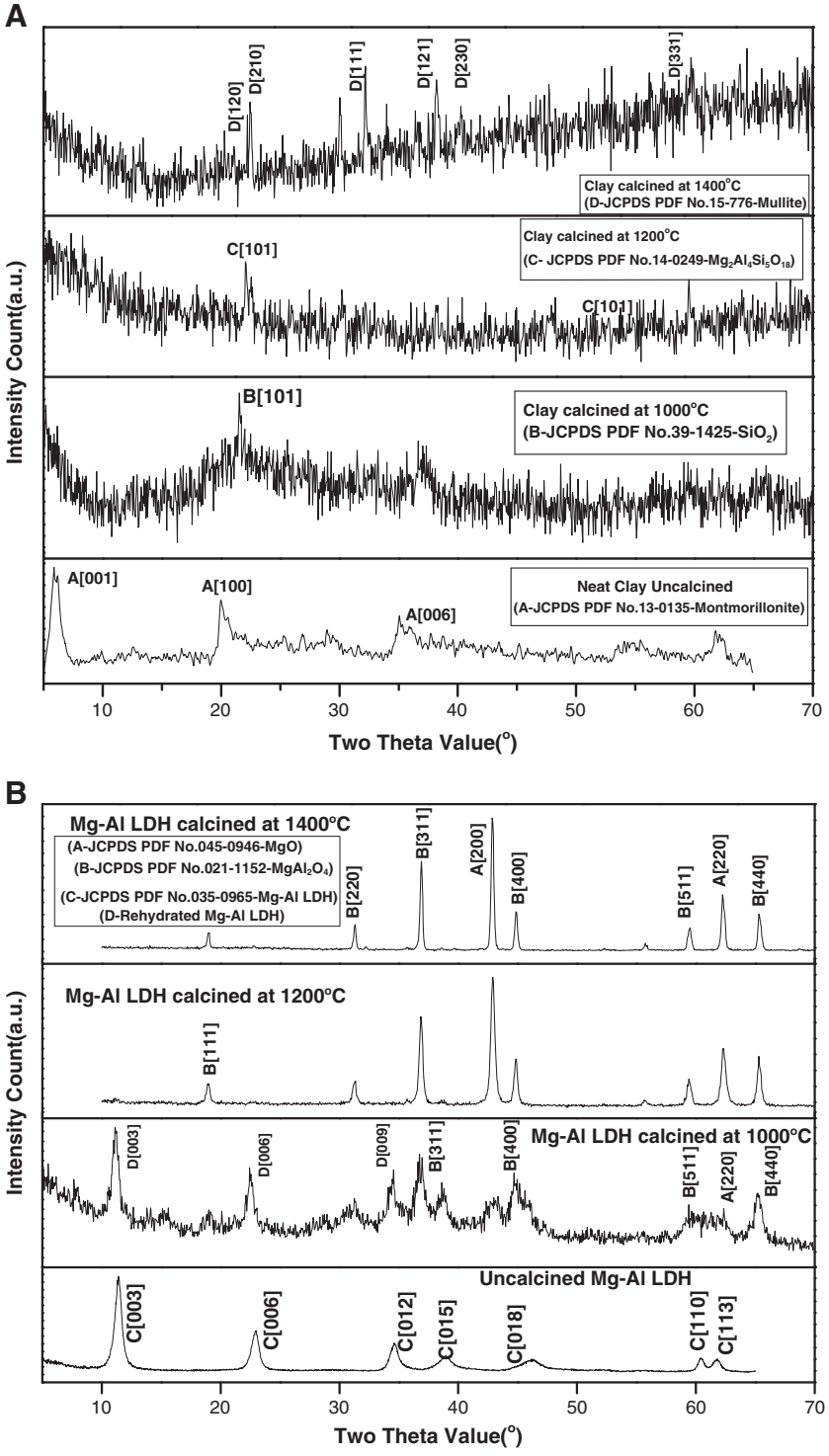

Fig. 2. The XRD patterns of A. Montmorillonite B. Mg–Al LDH, and C. Montmorillonite/LDH — calcined at different temperatures.

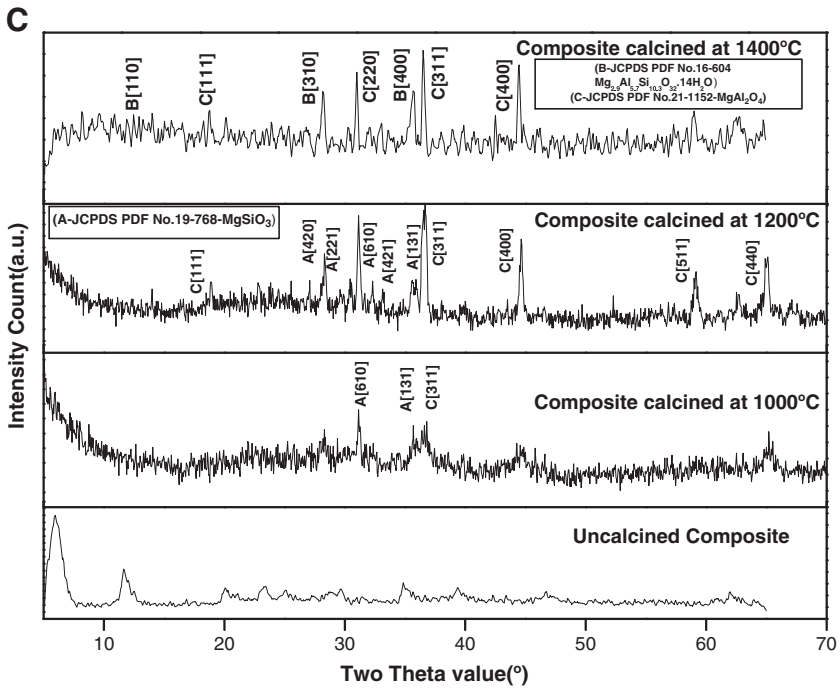

Fig. 2 (*continued*).

At dynamic measurements, the samples were heated in air at a heating rate of 10 °C/min using the DTA–TGA equipment SDT 2960 (from M/S TA Instruments USA).

2.1.6. Coating ceramic preforms with the gels

Prior to dip coating, the α-alumina tubes were washed with distilled water and dried in air at 110 °C for 2 h. Dip coatings was carried out by submersion and withdrawing the supports at different rates and different montmorillonite/LDH ratios (Fig. 1). The dip-coated tubes were dried overnight at room temperature followed by heating in air at 40° and 80 °C for 6 h. The thicknesses of the coats were varied by changing the solid content of the coating dispersions.

The α-Al_2O_3 tubes (manufactured by M/S Naskar Ceramics, Kolkata, India) had a wall thickness of 3.0 mm, a length of 35 mm and an internal diameter of 15 mm. For coating those dispersions were selected where the rheograms did not show any viscosity drop due to floc formation. The dried coatings were calcined in air up to 1400 °C at a heating profile of 5 °C/min. The calcined products were allowed to cool to room temperature under normal atmosphere within the furnace.

2.1.7. Mechanical properties of the coated bodies

The compressive and tensile strength of the coated bodies were measured using the compression platens and mechanical jaws of the Instron UTM machine equipped with the Merlin software version V22054. For compressive strength measurement coated α-alumina tubes of 35 mm length were used. For the measurement of the tensile extension cut out strips of longer α-alumina tubes with the approximate dimension of 15 cm length and 2 mm width were used.

3. Results and discussions

There was an initial sharp rise of the shear stress in the flow curves (Fig. 3) for the montmorillonite/LDH dispersions. This can be attributed to the force needed to break the network of montmorillonite and LDH particles (Fig. 1).The plateau of the flow curves in Fig. 4 had a maximum at the montmorillonite/LDH ratio 0.5:0.3 indicating the optimal ratio of the components. Similar behavior of destabilization due to heterocoagulation was reported earlier (Lagaly et al., 2001a, 2001b).

The electrokinetic mobility was always negative (Table 1). The numerical value decreased with increasing LDH content. Also, the negative value remained stable over the pH range of ≈6.0 to 9.0 because the positive charge of the LDH particles did not change much as well as the total negative charge of the montmorillonite particles. It was the effective negative potential that kept the composite particles dispersed.

The XRD pattern of the Na-montmorillonite heated at 1000 °C showed broad reflections corresponding to the formation of cristobalite (JCPDS PDF-39-1425). After calcination at 1200 °C, the

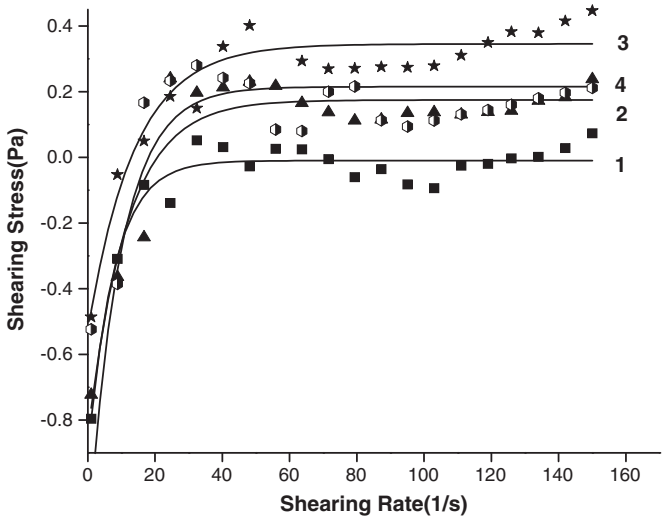

Fig. 3. Rheograms of different dispersions measured in Rheolab QC (1. 0.5% Na-montmorillonite, 2. 0.5% Na-montmorillonite + 0.1% Mg–Al LDH, 3. 0.5% Na-montmorillonite + 0.3% Mg–Al LDH, 4. 0.5% Na-montmorillonite + 0.35% Mg–Al LDH).

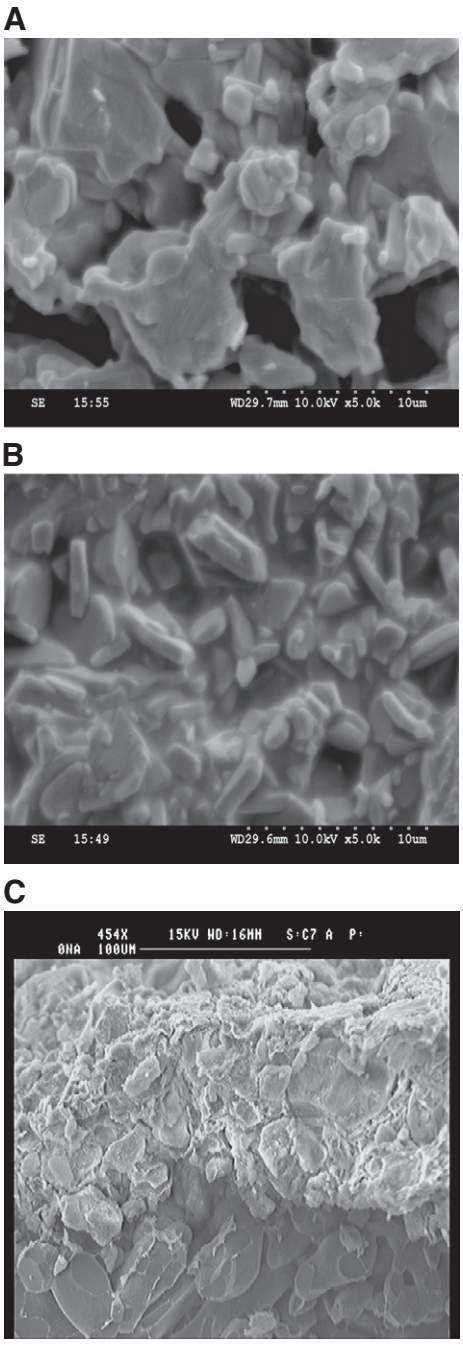

Fig. 4. SEM images of A. Uncoated support with voids of the dimension of about 30 μm; Coated support B. Surface View, and C. Edge View.

reflection of a Mg–Al silicate appeared (JCPDS PDF 14–249). At 1400 °C, mulite was formed (JCPDS PDF card No 15–776).

The powder XRD pattern of uncalcined Mg–Al LDH showed the reflections of hydrotalcite (JCPDS PDF card No 35–0965). Three crystalline phases were formed at 1000 °C (Fig. 2b): MgO, $MgAl_2O_4$ and rehydrated Mg–Al LDH. The rehydrated LDH was formed by the memory effect generally shown by this type of compounds (Miyata, 1980). The reflections corresponding to this rehydrated Mg–Al LDH were indexed with a hydrotalcite type structure using the PXRD data interpretational software POWD. Due to turbostratic distortions of the layers, an accurate determination of the cell parameters was difficult to achieve. However, with a = 3.1 Å and a three layered hexagonal cell system with c = 23.64 Å, a set of indexed planes were calculated (Fig. 2B).

Table 1
The electrokinetic mobility values of montmorrillonite/LDH at different pH and different Na-montmorillonite/LDH ratios.

Sl No.	Sample composition	Electrokinetic mobility (m^2/Vs)	pH
1	0.5% (m/v) Na-montmorillonite	−6.5	8.8
		−6.6	7.9
		−4.0	7.0
		−4.3	6.2
		−4.1	5.8
2	0.5% (m/v) Na-montmorillonite + 0.075% LDH	−3.4	9.9
		−3.1	8.9
		−2.9	7.8
		−2.8	7.0
		−1.8	6.1
3	0.5% (m/v) Na-montmorillonite + 0.2% LDH	−2.9	9.9
		−2.4	8.9
		−2.1	8.0
		−2.1	7.0
		−1.6	6.1
4	0.5% (m/v) Na-montmorillonite + 0.25% LDH	−2.7	9.9
		−2.2	9.0
		2.0	8.1
		−1.7	7.0
		−1.4	5.9
5	Mg–Al LDH	+3.6	6.4

The powder XRD patterns of Mg–Al LDH, heated to 1200 and 1400 °C, indicated sharp MgO and $MgAl_2O_4$ (Fig. 2B) reflections. On the other hand, in case of the composite gel, the MgO reflections were not observed after calcination above 1000 °C. At 1000 °C, the MgO began to react with the decomposed montmorillonite particles by forming crystalline $MgSiO_3$. In the XRD pattern of the composite calcined to 1400 °C the $MgSiO_3$ reflections disappeared after cooling to room temperature in air, and Mg $_{2.9}Al_{5.7}Si_{10.3}O_{32}.14H_2O$ was formed. This molten Mg $_{2.9}Al_{5.7}Si_{10.3}O_{32}.14H_2O$ probably solidified during cooling and cemented the $MgAl_2O_4$ particles like stones in a concrete mortar or glass ceramics. A similar observation of spinel formation in a vitrified matrix was reported in fly-ash calcination products (Frugier et al., 2002).

The formation of the aluminosilicate matrix containing well-grown cubical crystals was also seen in the SEM (Fig. 5A) images of the 1400 °C calcined gels. The EDXA pattern (Fig. 5B) of these cubical crystals showed them as composed of magnesium, aluminum and oxygen confirming the powder XRD pattern of the $MgAl_2O_4$ spinel. The presence of the aluminosilicate in the macropores of the alumina tubes was seen in the SEM (Fig. 4C) images. The bright spots in the AFM image of the composite heated at 1400 °C indicated the spinel crystals in the aluminosilicate matrix (Fig. 5C).

The DTA–TGA curves of Mg–Al LDH and montmorillonite/LDH showed four steps between 30 and 700 °C corresponding to the loss of adsorbed water (70–125 °C), the dehydroxylation of LDH (430–550 °C) and of montmorillonite (550–700 °C) (Fig. 6).

The peak at 840 °C in the DTA curve of Mg–Al LDH corresponds to the transition into an Mg–Al-oxide (Sato et al., 1987).

In the bar diagrams (Fig. 7), **A** represents the mechanical strength of the original α-alumina tubes, whereas **B** represents the mechanical strength of the same α-alumina tubes after calcination at 1400 °C, **C** represents the mechanical strength of the tube **B** after coating. Thus, coating with only Na-montmorillonite reduced the strength from ≈7960 N to 5930 N. When the tubes were coated with a gel containing montmorillonite and LDH in the ratio 1, the strength increased to 9090 N (Fig. 7D) and to 15,400 N when the montmorillonite/LDH ratio was 2 (Fig. 7E). The increased strength was basically due to the reinforcement of the strength inside the pores by the spinel particles.

Also, the extension (Fig. 8) in the z-direction was increased by 4%. Thus, the tensile extension data also corroborated the increase of the mechanical strength of the α-alumina tubes by infiltration of the

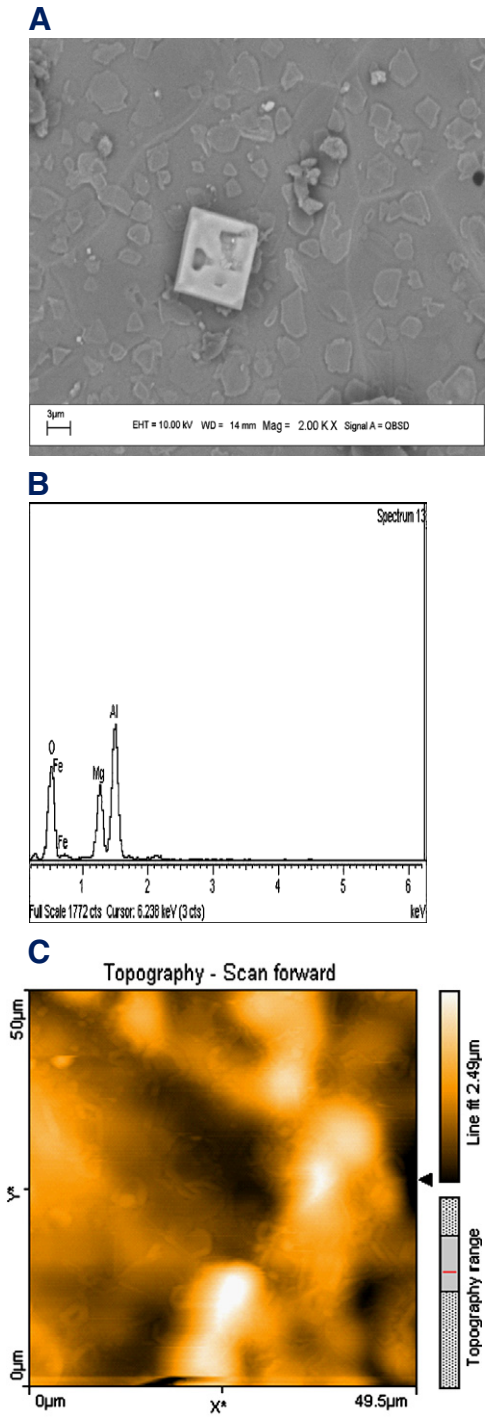

Fig. 5. (A) SEM image showing cubic spinel crystal dispersed in the aluminosilicate matrix after heating to 1400 °C, (B) the corresponding EDXA pattern (C) corresponding AFM image.

composite into the pores. The aluminosilicate and crystals of spinel particles formed a composite inside the pores, which was responsible for the improvement of the mechanical properties of the α-alumina tubes.

4. Conclusion

A major problem in ceramic matrix composite formation is processing of the components e.g. the preparation of Al_2O_3–ZrO_2 mixtures by conventional methods. When mixed in a ball mill, ZrO_2 crystallites are agglomerated leading to improper dispersion and poorer strength of the final ceramic material. In comparison to such mechano-chemical mixing of two solids, the study described the preparation of a composite gel. Coating alumina tubes with the composite gels provided the end products of improved mechanical strength which is expected to be advantageous. In such a case, the possibility of agglomeration in the green material can be controlled. Apart from this, the present approach uses economically cheaper materials (montmorillonite, Mg–Al LDH) compared to ZrO_2.

Therefore, in view of the different uses of Al_2O_3 ceramic materials e.g., in pump seals, wear plates for the industrial components, extrusion dies or bio inert materials in various orthopedic devices or ceramic membranes, the present approach can be expected to lead to future applications.

Acknowledgment

The authors thank Dr. P.G. Rao, Director, NEIST (formerly known as RRL), Jorhat for permission to carry out the work. The authors are also grateful to CSIR, New-Delhi (under Network project) as well as to the Ministry of Environment & Forests, Govt. of India (under Grant-in-Aid project) for the financial support.

References

Abend, S., Lagaly, G., 2000. Sol–gel transitions of sodium montmorillonite dispersions. Appl. Clay Sci. 16, 201–227.
Abend, S., Bonnke, N., Gutschner, U., Lagaly, G., 1998. Stabilization of emulsions by heterocoagulation of clay minerals and layered double hydroxides. Colloid Polym. Sci. 276 (8), 730–737.
Ariga, K., Lvov, Y., Ichinose, I., Kunitake, T., 1999. Ultrathin films of inorganic materials (SiO_2 nanoparticle, montmorillonite microplate, and molybdenum oxide) prepared by alternate layer by layer assembly with organic polyanions. Appl. Clay Sci. 15, 137–152.
Bain, D.C., Smith, B.F.L., 1994. Chemical analysis. In: Wilson, M.J. (Ed.), Clay Mineralogy: Spectroscopic and Chemical Determinative Methods, London, pp. 300–332.
Brindley, G.W., Brown, G., 1980. Crystal Structures of Clay Minerals and Their X-Ray Identification, Monograph No 5. Mineralogical Society, London.
Burba, III, J. L., Barnes, Audrey L., 1987. Mixed metal layered hydroxide-clay adduct as thickener for water and other hydrophylic fluids. U S patent 4664843.
Decher, G., Lvov, Y., Schmitt, J., 1994. Proof of multilayer structural organization in self assembled polycation–polyanion molecular films. Thin Solid Films 244, 772–777.
Forano, C., Hibino, T., Letoux, F., Taxiot-Gueho, C., 2006. Layered double hydroxides. In: Bergaya, F., Theng, B.K.G., Lagaly, G. (Eds.), Handbook of Clay Science. Elsevier, Amsterdam, The Netherlands, pp. 1021–1096.
Frugier, P., Godon, N., Vernaz, E., Larche, F., 2002. International congress waste stabilization & environment, 99. Waste Manag 22 (2), 137–142 Lyon, FRANCE.
Goswamee, R.L., Sengupta, P., Bhattacharyya, K.G., Dutta, D.K., 1998. Adsorption of Cr (VI) in layered double hydroxides. Appl. Clay Sci. 13, 21–34.
Goswamee, R.L., Ayral, A., Bhattacharyya, K.G., Dutta, D.K., 2009. A process for the preparation of active metal oxide composites useful as toxic gas adsorbent from mixed metal layered hydroxides and smectite clay. Indian patent No 235052.
Jones, W., Chibwe, M., 1989. The synthesis, chemistry and catalytic applications of layered double hydroxides. In: Mitchell, I.V. (Ed.), Pillared Layered Structures: Current Trends and Applications. Elsevier, London and New York, pp. 67–77.
Kovanda, F., Balek, V., Dornicak, P., Martinec, P., Maslan, M., Bilkova, L., Kolousek, D., Bountseva, M.I., 2003. Thermal behaviour of synthetic pyroaurite like anionic clay. J. Therm. Anal. Calorim. 71, 727–737.
Lagaly, G., 1999. Introduction: from clay mineral–polymer interactions to clay mineral–polymer nanocomposites. Appl. Clay Sci. 15, 1–9.
Lagaly, G., 2006. Colloid clay science. In: Bergaya, F., Theng, B.K.G., Lagaly, G. (Eds.), Handbook of Clay Science. Elsevier, Amsterdam, The Netherlands, pp. 141–246.
Lagaly, G., Mecking, O., Penner, D., 2001a. Colloidal magnesium aluminum hydroxide and heterocoagulation with a clay mineral. I. Properties of colloidal magnesium aluminium hydroxide. Colloid Polym. Sci 279, 1090–1096.
Lagaly, G., Mecking, O., Penner, D., 2001b. Colloidal magnesium aluminum hydroxide and heterocoagulation with a clay mineral. II. Heterocoagulation with sodium montmorillonite. Colloid Polym. Sci. 279, 1097–1103.
Lee, Y.-C., Kuo, C.-L., Wen, S.-B., Lin, C.-P., 2007. Changes of organo-montmorillonite by ball milling in water and kerosene. Appl. Clay Sci. 36, 265–270.
Li, S.P., Hou, W.G., Xiao, J.C., Hu, J.F., Li, D.Q., 2003. Influence of measuring conditions on the thixotropy of hydrotalcite-like/montmorillonite suspension. Colloids Surf., A Physicochem. Eng. Aspects 224, 149–156.
Li, L., Ma, R., Ebina, Y., Iyi, N., Sasaki, T., 2005. Positively charged nanosheets derived via total delamination of layered double hydroxides. Chem. Mater. 17, 4386–4391.
Miyata, S., 1975. The synthesis of hydrotalcite like compounds and their physico-chemical properties: I. The Systems Mg^{2+}–Al^{3+}–NO_3^-, Mg^{2+}–Al^{3+}–Cl^-, Mg^{2+}–Al^{3+}–ClO_4^-, Ni^{2+}–Al^{3+}–Cl^- and Zn^{2+}–Al^{3+}–Cl^-. Clays Clay Miner. 23, 369–375.

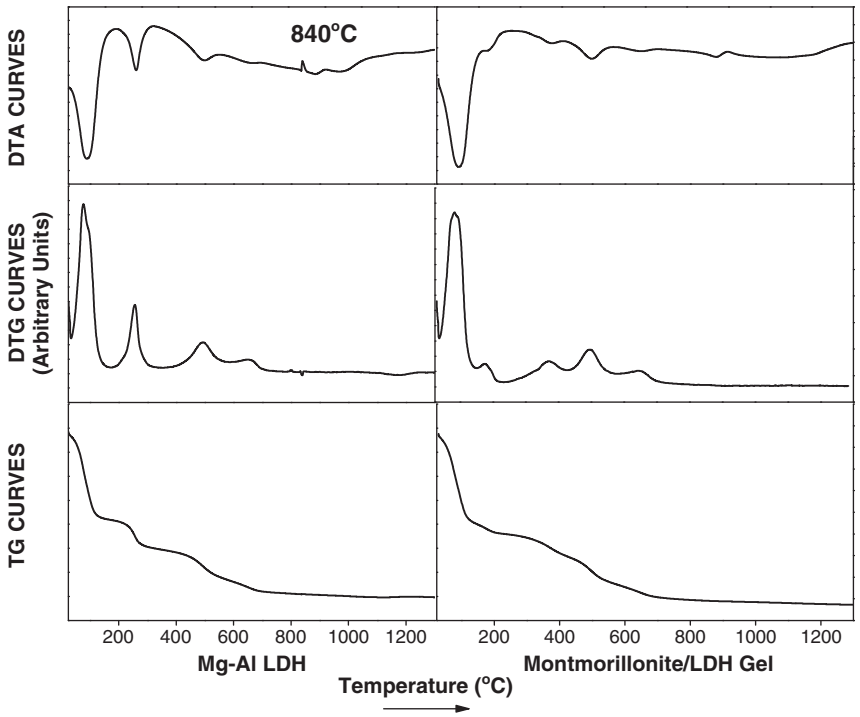

Fig. 6. TG, DTG, DTA curves A_1, A_2, A_3 = Mg-Al LDH and TG, DTG, DTA B_1, B_2, B_3 = montmorillonite/LDH.

Miyata, S., 1980. Physico-chemical properties of synthetic hydrotalcites in relation to composition. Clay Clay Miner. 28 (1), 52–56.
Patel, A.H., Somani, S.R., Bajaj, C.H., Jasra, V.R., 2007. Preparation and characterization of phosphonium montmorillonite with enhanced thermal stability. Appl. Clay Sci. 35, 194–200.
Sato, T., Tezuka, M., Endo, T., Shimada, M., 1987. Removal of sulfuroxyanions by magnesium aluminium oxides and their thermal decomposition. J. Chem. Technol. Biotechnol. 39, 275–285.
Searle, A.B., Grimshaw, R.W., 1960. The Chemistry and Physics of Clays and Other Ceramic Materialsthird ed. Ernest Benn Limited, London.
Sparling, D.P., Williamson, D., 1991. Mixed metal hydroxide mud improves drilling in unstable shales. Oil Gas J. 10, 29–34 June.
Taylor, H.F.W., 1973. Crystal structures of some double hydroxide minerals. Mineral. Mag. 39 (304), 377–389.
van Olphen, H., 1977. An Introduction to Clay Colloid Chemistrysecond ed. John Wiley & Sons, New York.
von Allmann, R., 1970. Doppelschichtstrukturen mit brucitaehnlichen Schichtionen $[Me(II)_{1-x}Me(III)_x\,(OH)_2]^{x+}$. Chimia. 24 (3), 99–108.

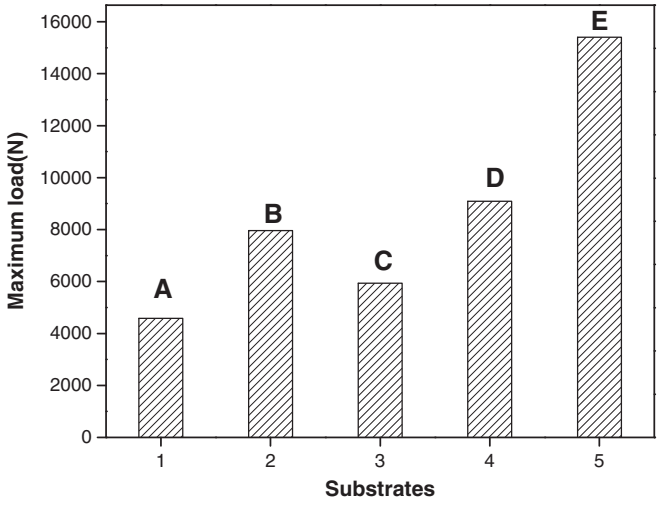

Fig. 7. Mechanical strength of uncoated and coated green and calcined α-alumina tubes: (A—green alumina tubes, B—uncoated calcined alumina tubes, C—calcined alumina tubes coated with only Na-montmorillonite, D—alumina tubes B coated with a 4% dispersion of Na-montmorillonite/LDH, mass ratio 1, E—calcined alumina tubes B coated with a 4% dispersion of Na-montmorillonite/LDH, mass ratio 2.

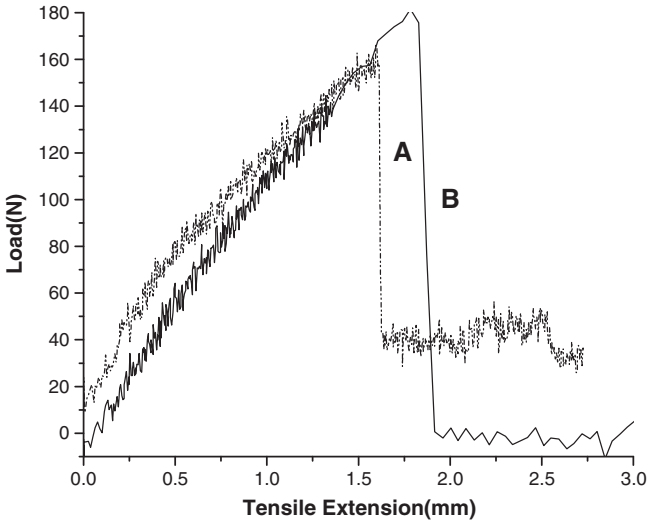

Fig. 8. Tensile extension against applied load A = uncoated calcined alumina tubes, B = coated calcined alumina tubes.